Ultrasonics Sonochemistry 76 (2021) 105655

Contents lists available at ScienceDirect

Ultrasonics Sonochemistry

journal homepage: www.elsevier.com/locate/ultson

# Resistant starch type 2 from lotus stem: Ultrasonic effect on physical and nutraceutical properties

Nairah Noor [a], Adil Gani [a,b,*], Faiza Jhan [a], Jenno J.L.H. [a], Mohd Arif Dar [c]

[a] Department of Food Science and Technology, University of Kashmir, Srinagar 190006, India
[b] Department of Food Science, Rutgers University, 65 Dudley Road, New Brunswick, NJ 08901, USA
[c] Department of Physics, Annamalai University, Annamalinagar, India

ARTICLE INFO

*Keywords:*
Resistant starch
Ultrasonication
Glycemic index
Anti-oxidant

ABSTRACT

Resistant starch type 2 (RS) was isolated from lotus stem using enzymatic digestion method. The isolated RS was subjected to ultrasonication (US) at different sonication power (100–400 W). The US treated and untreated RS samples were characterized using dynamic light scattering (DLS), scanning electron microscopy (SEM), light microscopy and Fourier transform infrared spectroscopy (FT-IR). DLS revealed that particle size of RS decreased from 12.80 μm to 413.19 nm and zeta potential increased from −12.34 mV to −26.09 mV with the increase in sonication power. SEM revealed smaller, disintegrated and irregular shaped RS particles after ultrasonication. FT-IR showed the decreased the band intensity at 995 $cm^{-1}$ and 1047 $cm^{-1}$ signifying that US treatment decreased the crystallinity of RS and increased its amorphous character. The bile acid binding, anti-oxidant and pancreatic lipase inhibition activity of samples also increased significantly ($p < 0.05$) with the increase in sonication power. Increase in US power however increased the values of hydrolysis from 23.11 ± 1.09 to 36.06 ± 0.13% and gylcemic index from 52.39 ± 0.38 to 59.50 ± 0.11. Overall, the non-thermal process of ultrasonic treatment can be used to change the structural, morphological and nutraceutical profile of lotus stem resistant starch which can have great food and pharamaceutical applications.

## 1. Introduction

Resistant starch is considered as a fraction of starch which is resistant to pancreatic α-amylase hydrolysis and as such remains undigested in small intestine but makes its way to the large intestine, where it acts as substrate (prebiotic) for gut microbiota [1-3]. The beneficial effects of resistant starch on fatty acid (FA) metabolism, inflammation reduction and glycemic control have been observed in both healthy as well as unhealthy subjects [4,5]. The fermentation of resistant starch in colon produces metabolites like short chain fatty acids (SCFAs) which can regulate glucose homeostasis, prevent colon cancer from red meat, elevate levels of satiety and increase post-prandial lipid oxidation [6]. On the basis of their structural characteristics, chemical modification, the impact of cooking, or association with lipids, scientists have divided resistant starch into five categories (RS1, RS2, RS3, RS4 and RS5). Because of the variation in composition, structure and effects due to various processing techniques, each type needs to be considered individually. In this study, RS2 has been chosen for analysis. RS2 is considered as uncooked starch having non-gelatinized granules. These have B- or C- polymorph crystallinity which makes these granules resistant to enzymatic hydrolysis [7]. The anti-digestibility of type 2 has recently received a considerable attention as the slow digestion of starch may lower the diet –related health complications including type-2 diabetes, colorectal cancers and obesity [8]. However the disadvantage associated with resistant starch is that it loses its enzymatic resistance upon heat based processing techniques as the latter cause's disruption of starch granules, melting of crystallites, creation of new helical structures and molecular breakdown [9]. The emerging food processing techniques including low pressure plasma, high hydrostatic pressure, pulsed electric field and ultrasound have gained an increasing attention owing to their ability to improve nutritional value and sensory attributes of foods [10].

One of these emerging techniques i.e. ultrasound (US) is a highly efficient, eco-friendly and safe technique which can be applied easily [11]. US treatment can affect the physicochemical and functional properties of starch coming from different botanical origins [12]. US treatment can modify the amorphous and crystalline domains of starch and thereby alter the digestibility, thermal and functional properties for different starches such as pea starch, foxtail millet starch and waxy corn

* Corresponding author at: Department of Food Science and Technology, University of Kashmir, Srinagar 190006, India.
*E-mail address:* Adil.gani@gmail.com (A. Gani).

https://doi.org/10.1016/j.ultsonch.2021.105655
Received 18 February 2021; Received in revised form 21 June 2021; Accepted 24 June 2021
Available online 29 June 2021
1350-4177/© 2021 Published by Elsevier B.V. This is an open access article under the CC BY-NC-ND license (http://creativecommons.org/licenses/by-nc-nd/4.0/).

starch [13,14]. For instance, US treatment increased the amylose content, damaged the crystal structure, favoured the starch-lipid complex formation and decreased the mean volume diameter [15]. Furthermore, the extent of cavitations, frequency, sonication power, amount of energy input and duration of treatment decides the effect of US treatment. US treatment increases the porosity of the starch which increases its surface area and in turn increases the chemical reactivity of starch molecules for further reactions [16]. In the view of current literature, there are a lot of publications highlighting the effect of US treatment on various kinds of starches, whereas no study investigating the effect of US –treatment on structural, morphological, functional and nutraceutical properties of RS2 ingredient has been reported. As to how US treatment impacts the structural, functional and nutraceutical properties of RS2, remains unclear. So RS2 isolated from lotus stem (*Nelumbo nucifera*) has been chosen for this study. *Nelumbo nucifera* belongs to family Nelumbonaceae and is an important freshwater aquatic plant in which starch forms about 70% of the dry weight of rhizomes and seeds [17]. The edible parts of the plant including buds, rhizome, seeds, flowers and leaves have been used in Asian traditional medicines to treat various disorders like hypertension, depression, vomiting, heart problems, diarrhoea, insomnia and cancer [17]. The present study therefore aimed at isolating RS2 from lotus stem and investigating the changes in particle size, chemical groups, granule morphology, functional properties, antioxidant potential, bile acid binding, pancreatic lipase inhibiting ability and in vitro glycemic index of RS2 under different US power. Dynamic light scattering (DLS), Fourier transform-infrared (FT-IR) spectroscopy, scanning electron and microscopy (SEM) and light microscopy were used to elucidate the structure of untreated and US-treated resistant starch. Effect of US treatment on water and oil absorption activity, apparent amylose content and freeze thaw stability was also evaluated. Nutraceutical potential of untreated and US- treated resistant starch was analyzed in terms of antioxidant potential, pancreatic lipase inhibiting activity and in vitro glycemic index. The new knowledge gains from study can establish RS2 as the ingredient in functional foods formulated for diabetic and obese people.

## 2. Materials and methods

### 2.1. Materials

The indigenous variety of lotus stem was procured from the local market of Srinagar, Jammu and Kashmir, India. The chemicals used were purchased from Sigma Aldrich (USA). The important chemicals used in the study were amylase from porcine pancreas, amyloglucosidase from *Aspergillus niger*, lipase from porcine pancreas and protease from *Bacillus Licehnformis*. All other chemicals used were of analytical grade.

### 2.2. Extraction of starch from lotus stem

The lotus stems were cleaned off dirt by washing these in chilled water. The stems were cut into small pieces and pulverized along with water in a domestic blender for 5 min. The starch was then extracted using alkaline steeping method as described by Ahmad et al. [18].

### 2.3. Extraction of resistant starch type 2 (RS) from starch

The extraction of RS from lotus stem was carried out using the method of Gani et al. [19] with slight modifications. Native starch weighing 5 g was added with 10 mL phosphate buffer (0.2 M, pH 5.2) in a dry centrifuge tube and voretexed for 5 min. This was followed by addition of 5 mg of protease to digest any residual protein. The enzyme mixture was vortexed for 2 min and kept on a water bath for 1 h at 37 °C. After incubation, the mixture was centrifuged at 2850 rpm for 10 min. The recovered pellet was washed with ethanol (99%) to inactivate any residual enzyme and treated with pancreatic lipase to digest the traces of lipids which may interact with amylose to form amylose lipid complex (RS type 5). The enzyme solution was made by dissolving 5 mg of porcine pancreatic lipase in 10 mL of buffer (100 mM PBS and NaCl (0.5%), pH 7.2). This enzyme mixture was again kept on a water bath at 37 °C for 1 h followed by centrifugation (2850 rpm for 10 min) and washing with 99% ethanol. The recovered pellet was then treated with pancreatic α-amylase enzyme solution (10 mg/mL having an activity of 25 U/mL) and 3.2 mL of amyloglucosidase (3U/ml) prepared in 250 mL of 0.1 M sodium acetate buffer, pH 5.2 to hydrolyse the digestible starch. The reaction mixture was kept on shaking water bath for 16 h at 37 °C. The starch suspensions were taken out and centrifuged (3000 rpm for 10 min). The obtained residues were subjected to repeated washing with 99% ethanol followed by washing with 50% ethanol. The resulting starch precipitates (RS) were then dried at 45 °C, ground and stored in air tight container for further analysis.

### 2.4. Ultrasonic treatment of resistant starch

The isolated RS (10 g) was suspended in 10 mL distilled water to make the final concentration of 10% (w/v). The prepared samples were stirred constantly on a magnetic stirrer for 10 min at room temperature. The suspensions were subjected to an ultrasonic probe sonicator (Cole-Parmer, 04711–35) at various ultrasonic powers (100, 200, 300 and 400 W). The recommended maximum frequency for the instrument was 20 KHz and sonication was carried at the same frequency. The diameter of probe was 12 mm. The pulse mode was 1 s on /1s off for the total processing time of 35 min. The treatment was carried out in an ice bath. The US treated RS solutions were then brought to room temperature and washed with distilled water by subjecting them to centrifugation for 15 min at 3500 rpm. Finally the US –treated RS pellets were freeze dried for 24 h and stored in air tight pouches at 4 °C for further analysis. The samples prepared at different sonication powers of 100, 200, 300 and 400 W were designated as URS1, URS2, URS3 and URS4, respectively.

### 2.5. Measurement of resistant starch.

The RS content of US- treated and untreated samples was estimated using the Megazyme Assay Kit (Megazyme International, Wicklow, Ireland), following the AACC protocol [20]. 100 mg of each sample was added with 4 mL of pancreatic α-amylase (25 U/mL) and 0.1 mL amyloglucosidase (3 U/mL). The enzyme-sample solutions were vortexed for 5 min and kept on shaking water (200 S /min) at bath for incubation 37 °C for 16 h. The RS solutions were then added with 4 mL ethanol to deactivate enzymes. This was followed by centrifugation (3500 rpm, 10 min) and the recovered pellet was washed twice with 50% ethanol to remove hydrolysed starch. The pellet was the dispersed into 2 mL of 2 M KOH by vigorous stirring for 20 min. The solutions were neutralized using sodium acetate buffer (8 mL, 1.2 M) and added with 0.1 mL amyloglucosidase (3300 U/mL), followed by incubation at 50 °C for 30 min. The samples were centrifuged (3000 rpm, 10 min) and 0.1 mL of aliquots from supernatant were taken and added with 3 mL of GOPOD followed by incubation for 20 min at 50 °C. Finally the absorbance was measured at 510 nm. RS was calculated as the amount of glucose × 0.9.

### 2.6. Particle size distribution

The average particle size and zeta potential of RS and US-treated RS samples were measured by using a Zeta sizer (Litesizer 500 Anton Paar, Austria). The samples weighing 0.01 gm were dispersed into 100 mL of milli-Q water (Elix-10, Millipore, Molsheim, France) using a sonicator bath at 40 KHz for few minutes. Approximately 3 mL of this dispersion was filled in a cuvette and monitored on Zeta sizer. For measuring the zeta potential, 0.01% (w/v) of the sample in KCl (0.1 mM) with pH near to neutral was kept for equilibration overnight before measurement. The measurements were carried out at 25 °C at neutral pH.

### 2.7. Scanning electron microscope (SEM)

The morphological changes brought by ultrasonication were analyzed using SEM (ZEISS EVO18 MODEL). The samples were mounted on a stub using a double sticky tape and coated with the thick film of gold. The analysis was carried under low vacuum at an accelerating voltage of 20 KV.

### 2.8. Light microscopy analysis

Samples were suspended in glycerol/water mixture (1, 1 V/V) and a drop of suspension was observed under a light microscope at 40x (LMI, Leedz Micro Imaging Ltd, UK).

### 2.9. Structure analysis by ATR-FTIR spectroscopy

The ATR-FTIR spectra of samples were recorded using FTIR spectrometer system (Cary 630 FTIR, Agilent Technologies, USA). The spectra was measured between the range of 550–4000 $cm^{-1}$ at room temperature. The spectra were examined using Resolution Pro software version 2.5.5 (Agilent Technologies USA).

### 2.10. Functional properties

#### 2.10.1. Water absorption and oil absorption capacity

Functional properties including water absorption capacity (WAC) and oil absorption capacity (OAC) of samples were evaluated using the method described by Ahmed et al. [21]. 2 g of samples on dry basis were placed in a pre weighted centrifuge tubes and mixed with 25 mL of distilled water/ mustard oil. The tubes were stirred for 30 min at 25 °C. This was followed by centrifugation carried out at 5000 rpm for 15 min (5810R, Eppendorf, Hamburg, Germany). The supernatant was discarded and the tubes were weighed again. The gain in weight was expressed as percentage of water/oil absorption.

#### 2.10.2. Freeze thaw stability

The freeze thaw stability of samples was determined according to the method given by Ashwar et al. [22]. 5 g of treated and untreated RS samples were dispersed in 100 mL of distilled water and heated on a water bath kept at 90 °C for 30 min. The gels obtained were kept under refrigeration for 16 h at 4 °C. This was followed by freezing the gels at −16 °C for 24 h. The frozen gels were thawed at 25 °C for 6 h and again frozen at −16 °C. The freeze thaw cycles were carried out for five times and for each cycle, the tubes were centrifuged at 1000g for 20 min at 10 °C. The % release of water was noted as freeze thaw stability.

### 2.11. Effect of ultrasonication on antioxidant potential

#### 2.11.1. DPPH (1, 1-diphenyl-2-picrylhydrazyl) radical scavenging activity

DPPH (1, 1-diphenyl-2-picrylhydrazyl) radical scavenging activity of samples was determined according to the method of Jhan et al. [23].

#### 2.11.2. Metal chelating ability

Metal chelating ability of US-treated and untreated samples was determined according to the method of Shah et al. [24].

### 2.12. Effect of ultrasonication on in vitro glycemic index

The in vitro starch hydrolysis and predicted GI of samples was estimated using the method of Reshmi et al. [25]. The released glucose after following the assay was noted using glucose oxidase peroxidase (GOD-POD) kit (K-GLOX, Megazyme Bray, Co. Wicklow, Ireland). The absorbance of samples was measured at 510 nm using D-glucose as standard. Finally the hydrolysis index was calculated as the percentage of total amount of glucose released in the time interval (0–180 min) as compared to that released from standard glucose over the same time duration.

Hydrolysis % or D-Glucose (μg/0.1 mL) = Absorbance sample/ Absorbance standard × 100

The glycemic indices (GI) of the samples were calculated using the equation of Goni et al. [26].

$pGI = 39.71 + 0.549HI$

### 2.13. Effect of ultrasonication on bile acid binding capacity.

The bile acid-binding capacity of US treated and untreated samples was determined using colorimetric method described by Ashwar et al. [22]. For this, 30 mg of samples were placed in a test tube and added with 10 mL of cholic acid solution (prepared by dissolving 200 mg cholic acid in 4.7 mL of 0.1 N NaOH). The mixture was stirred on a magnetic stirrer for 2 h at 37 °C. After stirring, the mixture was filtered through 0.2 mm syringe filter. The filtered solution measuring 1 mL was added with 1 mL 0.9% alcoholic furfural solution and 5 mL of 16 N sulphuric acid. The reaction mixture was first kept on an ice bath for 15 min and then kept on water bath at 75 °C for 8 min, then again on an ice bath for 2 min. Finally the absorbance was measured at 490 nm.

### 2.14. Effect of ultrasonication on pancreatic lipase (PL) inhibition activity

The Pancreatic lipase inhibition assay was carried out using the colorimetric method described by Badmaev et al. [27] with some modifications. The substrate used in the assay was p-nitrophenol butyrate (pNPB). The assay mixture consisted of 50 μL of samples and 25 μL of pNPB (10 mM). The mixture was pre-incubated for a period of 10 min followed by the addition of pancreatic Lipase enzyme solution (50 mg/mL) prepared in sodium phosphate buffer (0.2 M; pH 7.2). The mixture was again incubated for 30 min at 37 °C. The released p-nitrophenol was estimated at 405 nm. The percentage of enzyme inhibition was calculated using the following equation:

$$\%Inhibition = \left(1 - \left(\frac{C-D}{A-B}\right)\right) * 100$$

Where,

A (Control) is the absorbance of without test sample but in the presence of enzyme

B (Control blank) is the absorbance without test sample and enzyme

C (Reaction) is the absorbance of test sample and enzyme

D (Reaction blank) is the absorbance with test sample but without enzyme.

### 2.15. Statistical analysis

The data reported are averages of triplicate observations. An analysis of variance with a significance level of 5% was done and Duncan's test applied to determine differences between means using the commercial statistical package (SPSS 16.0).

## 3. Results and discussions

### 3.1. Particle size, polydispersity index and zeta potential

The particle size, polydispersity index (PDI) and zeta potential of samples is presented in Table 1. The hydrodynamic diameter of RS was observed to be 12.80 μm whereas the increase in US power from 100 to 400 W resulted in decrease of particle dimensions. The corresponding values for US treated samples showed the values of 765.11 nm, 544.32 nm, 413.19 nm and 385.69 nm for the US power of 100, 200, 300 and 400, respectively. Previous study by Ogutu [28] also displayed that US treatment can reduce the molecular weight and particle size of sweet-potato pectin. The effect of US on the structure of starch is mainly caused by the collapse of bubbles generated by the ultrasound wave moving

**Table 1**
Particle size, polydispersity index and zeta potential of untreated and US- treated resistant starch from lotus stem.

| Sample | Power (W) | Hydrodynamic diameter | Polydispersity index (PI) | Zetapotential (mV) |
|---|---|---|---|---|
| RS | – | 12.8 ± 0.09 μm | 0.543 ± 0.34 | −12.34 ± 0.38 |
| URS1 | 100 W | 765.11 ± 0.78 nm | 0.413 ± 0.01 | −14.09 ± 0.42 |
| URS2 | 200 W | 544.32 ± 1.23 nm | 0.400 ± 0.05 | −18.67 ± 0.01 |
| URS3 | 300 W | 413.19 ± 0.03 nm | 0.342 ± 0.01 | −20.18 ± 0.32 |
| URS4 | 400 W | 385.69 ± 0.15 nm | 0.310 ± 0.32 | −26.09 ± 0.99 |

Where PI = Polydispersity index; RS is the resistant starch from lotus stem; US is ultrasonication; URS1, URS2, URS3 and URS4 represent the resistant starch ultrasonicated at 100, 200, 300 and 400 W.

through an aqueous medium [29]. The phenonmenon is termed as cavitation and results in breakage of polymer chains and induction of polymer degradation [30].

Moreover, PDI of RS (0.543) also displayed a decrease in the value with the increase in US power. The lower values of PDI (i.e. i ≤ 0.4) indicate homogeneity of particles and narrow particle size distribution [31]. The net charge on all the samples was negative which could be due to naturally occurring phosphate esters in amylopectin molecules [32]. The zeta potential of RS was −12.34 mV whereas the US treated samples showed significantly higher zeta potential. The corresponding values of zeta potential for samples treated with US power of 100, 200, 300 and 400 were found to be −14.09 mV, −18.67, −20.18 and −26.09, respectively. The increase in zeta potential may be attributed to the increase in anionic charge (hydroxyl groups) on the surface resulting from the degradation of polymer matrix due to US treatment [33]. The higher values of zeta potential for US treated samples indicate higher electrostatic repulsion between particles. The higher the electrostatic repulsion, lower will be the Van der Waals forces. Since Van der Waals forces are responsible for agglomeration of particles, therefore a decrease in these forces will increase the stability of sonicated RS particles [34]. The zeta potential of −20 mV for biopolymers may offer sufficient stability to them due to the stabilization of steric parameters [35]. Thus US treatment resulted in reduction of particle size with narrow particle size distribution and higher surface charge for RS particles isolated from lotus stem.

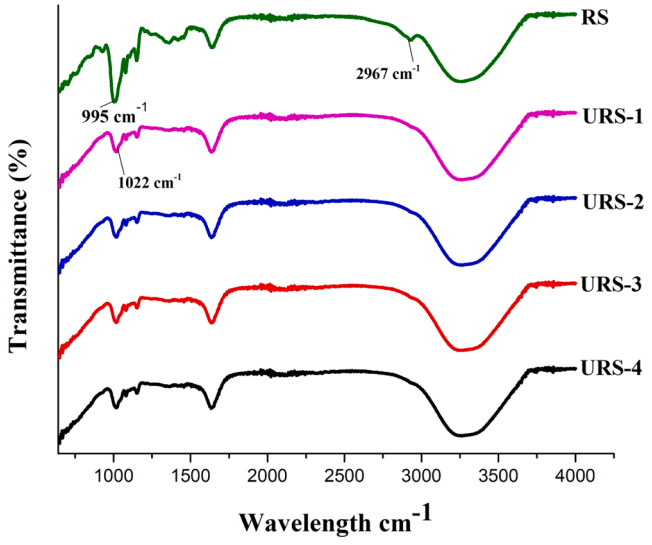


**Fig. 1.** FTIR spectra of untreated and ultrasonication treated resistant starch from lotus stem. Where URS-1, URS-2, URS-3 and URS-4 are the samples of resistant starch (RS) ultrasonicated at 100, 200, 300 and 400 W, respectively.

### 3.2. Fourier transform infrared spectroscopy (FTIR)

The results of FT-IR spectra are displayed in Fig. 1. RS displayed strong C–H and C–O stretching at 2926 $cm^{-1}$ and 1695 $cm^{-1}$ which may be due to the assembly of amylose helices during enzymatic treatment. Our results are in line with the study by Ma et al. [36] who reported a similar C–C, C–OH, and C–H stretching vibrations of the resistant starch isolated from Liard lentils. The bands at 995 $cm^{-1}$ and 1047 $cm^{-1}$ correspond to the ordered and crystalline structure of RS whereas the bands at 1022 $cm^{-1}$ correspond to the amorphous and disordered ordered structure [37]. For RS, the bands at 995 $cm^{-1}$ and 1047 $cm^{-1}$ had maximum stretching whereas for US treated samples, the increase in US power decreased the band intensity at 995 $cm^{-1}$ and 1047 $cm^{-1}$ signifying that US decreased the crystallinity of RS and increased its amorphous character. Furthermore the bands at 2926 $cm^{-1}$ representing the C–H stretching vibrations decreased as sonication power increased from 100 to 400 W. The percent transmittance of US treated samples decreased with the increase in sonication power. Overall the chemical groups in all the samples displayed no major change, showing that US had no major effect on the chemical structure of RS.

### 3.3. Morphology

The surface morphology of RS and US-treated samples was analyzed using scanning electron microscopy (SEM) and light microscopy. As shown in Fig. 2(A), RS displayed rough surface with irregular matrix. The surface appeared to be smooth and fissure free. US treated samples Fig. 2(B- E) displayed disintegrated, small and irregular particles. The application of ultrasound resulted in breakdown of RS matrix and the distortion of granule surface. The degradation of RS particles increased as the sonication power increased. In our study, US treated samples retained most of the surface characteristics of RS, fragmentation was the only visible change seen. The sonic energy trapped by RS granules produce high-frequency vibrations which break the RS matrix. Similar observations were also reported by Yongbo et al. [38] who reported no major difference in the microstructures among US treated and untreated resistant starch type 4.

Light microscopy also displayed irregular arrangement of RS particles (Fig. 3A) which was consistent with SEM observation (2A). This solid aggregation of RS crystallites offers resistance against enzyme attack [39]. As shown in Fig. 3B to E, US treated samples displayed disintegrated appearance. The fragments became smaller as the US power increased.

### 3.4. Apparent amylose content (AAC) and total resistant starch content (TRC)

The values of AAC (%) and TRC (%) for US treated samples were significantly higher ($p < 0.05$) than untreated RS. The values for US treated samples increased significantly ($p < 0.05$) with the increase in US power. The highest value for ACC and TRC was observed for URS4 with the corresponding values of 49.10 ± 0.43% and 96.23 ± 1.11%. The values for other samples are presented in Table 2. The increase in ACC may be due to the release of linear chains of amylose as a result of cavitations, mechanical shear force and shock waves caused by US treatment [40]. An increase in amylose content of *Radix Puerariae* starch after using high-intensity low-frequency US was also reported by Li et al. [41]. The digestibility properties of starch are greatly affected even by the small differences in amylose content [42]. The significant increase ($p < 0.05$) in resistant starch content with the increase in US power can be attributed to the high amylose content. There is a positive relation between amylose content and RS content. More the amylose content more will be resistant starch content of the sample [43]. Gani et al. [19] also reported that high values of amylose content were a contributing factor to high RS content of rice cultivars and horsechestnut.

High amylose content tends to increase resistant starch and the

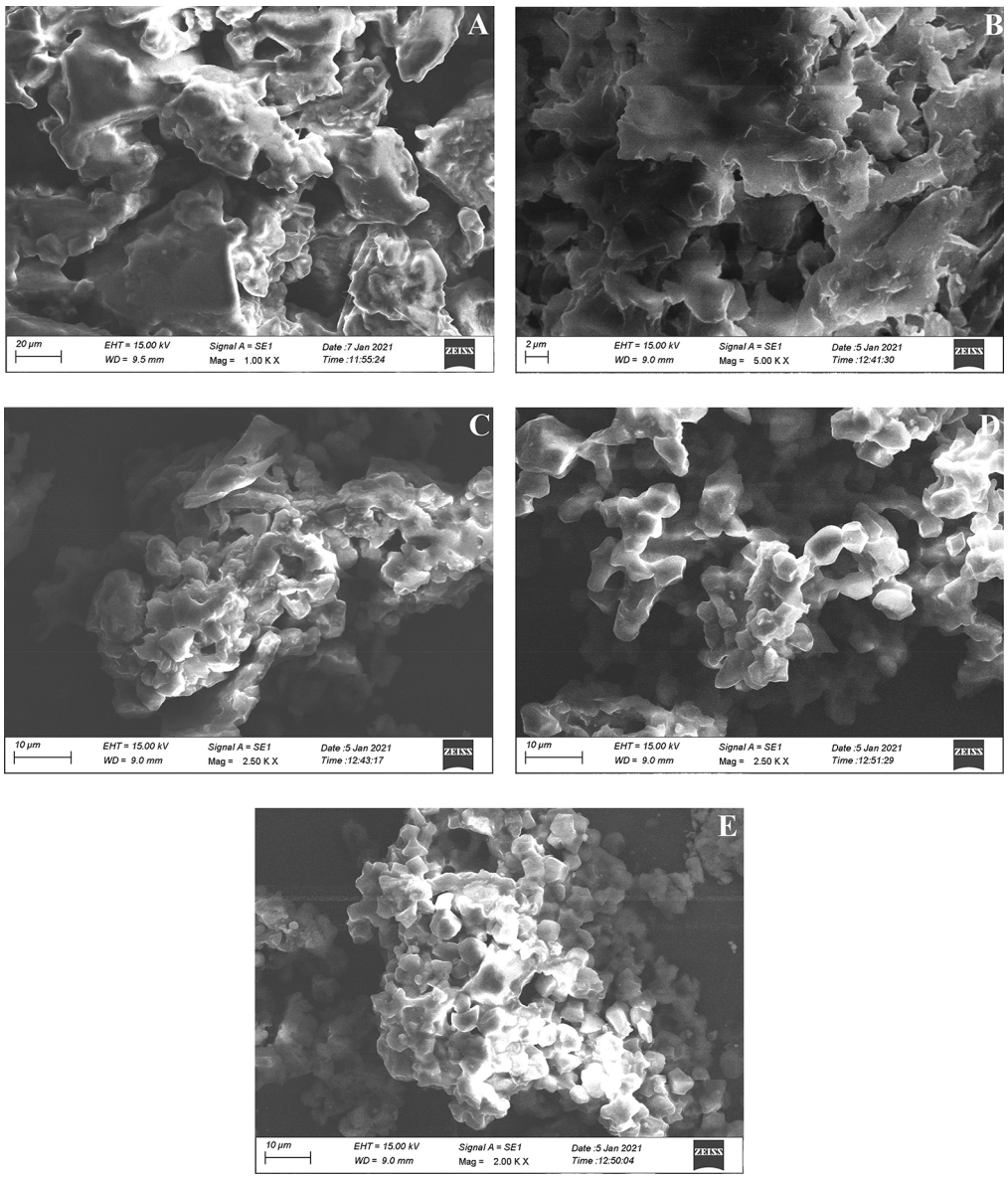


**Fig. 2. (A-E)**. Representative scanning electron microscopy of RS (A), RS ultrasonicated at 100 W (B), RS ultrasonicated at 200 W (C), RS ultrasonicated at 300 W (D) and RS ultrasonicated at 400 W (E). RS is the resistant starch isolated from lotus stem.

reason might be that during the gelatinization process, starch granules absorb water and swell and the amylose leaches out of swollen granules [44]. Following the retrogradation, amylose is the first candidate to recrystallize forming a more tightly packed crystalline structure, which is difficult for enzymes to hydrolyze. So as the amylose content will increase, tightly packed crystals upon retrogradation will produce higher levels of RS which also results in increase in the degree of crystallinity [45]. Also the amylose strands may realign to form double helices stabilized by hydrogen bonds, which can lead to further formation of resistant starch [46].

### 3.5. Water absorption capacity (WAC) and oil absorption capacity (OAC)

The results of WAC and OAC are shown in Table 3. WAC and OAC of URS1, URS2, URS3, and URS4 were significantly different ($p < 0.05$) than RS and the values increased with the increase in US power (100–400 W). The WAC of RS was found to be $0.50 \pm 0.76$ g/g, whereas the values of US-treated samples increased from $1.23 \pm 0.98$ to $3.53 \pm 1.12$ g/g. The possible reason for the increase in WAC of US treated samples might the breakdown of crystalline molecular structure of RS and binding of the water molecules to the free hydroxyl groups of amylose and amylopectin via hydrogen bonds. US results in dissociation of short range ordered structure and physical damage of starch molecules which results in binding of free hydroxyl groups of water and starch via hydrogen bridge, thereby enhancing the WAC of starch [47]. Similar results have also been reported in wheat, rice, waxy and normal maize starch [30].

OAC of gives us an idea about the oil binding capacity of resistant starch under particular conditions. OAC increased significantly ($p < 0.05$) with the increase in US power. In our study, OAC of RS was found to be $0.22 \pm 0.76$ g/g whereas the values of OAC for US treated samples increased from $1.09 \pm 0.23$ to $2.93 \pm 0.24$ g/g with the increase in sonication power. The physical entrapment of oil inside the starch matrix or inside the helical structures formed by amylose or amylopectin (amylose–lipid complexes) is due to the capillary forces [48]. There is a possibility that increase in pore size and volume of RS due to ultrasound may allow for more oil binding. Similar results were also observed by

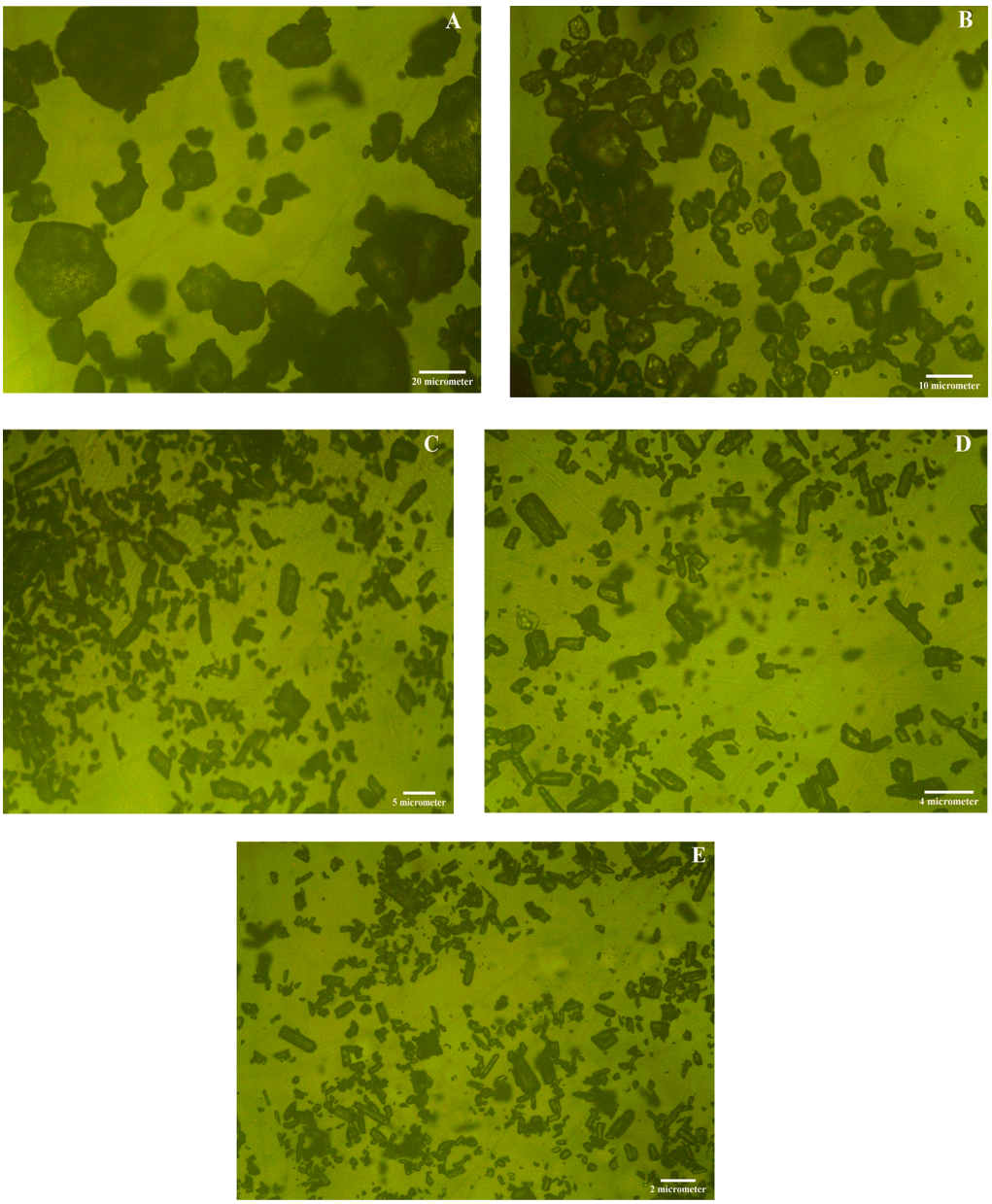


**Fig. 3. (A-E)**. Representative light microscopy images (magnification, 40x) of RS (A), RS ultrasonicated at 100 W (B), RS ultrasonicated at 200 W (C), RS ultrasonicated at 300 W (D) and RS ultrasonicated at 400 W (E). RS is the resistant starch isolated from lotus stem.

**Table 2**
ACC (%) and TRC (%) of untreated and US-treated resistant starch from lotus stem.

| Sample | | ACC (%) | TRC (%) |
|---|---|---|---|
| RS | | $41.87 \pm 1.23^{a}$ | $88.24 \pm 0.09^{a}$ |
| URS1 | 100 W | $43.09 \pm 0.43^{b}$ | $91.54 \pm 2.10^{b}$ |
| URS2 | 200 W | $45.23 \pm 1.09^{c}$ | $93.20 \pm 0.87^{c}$ |
| URS3 | 300 W | $48.09 \pm 0.56^{d}$ | $93.11 \pm 0.32^{c}$ |
| URS4 | 400 W | $49.10 \pm 0.43^{d}$ | $96.23 \pm 1.11^{d}$ |

Where ACC is apparent amylose content; TRC is total resistant starch content; US is ultrasonication; URS1, URS2, URS3 and URS4 represent the resistant starch ultrasonicated at 100, 200, 300 and 400 W. The results are the means of three replications ± standard deviations. Means in the column with different superscript differ significantly ($p > 0.05$).

Rashmi Singh et al. [49].

The effect of increasing the polarity (WAC) on OAC needs to be elaborated. Oil absorption capacity of starch is mainly due to its ability to physically bind oil due to capillary attraction as it does not possess non polar sites like protein [50]. So the increase in OAC capacity may be assumed to be a physical change which is brought up by degradation of cross linked starch that increases the pore size and allows more oil to be entrapped. Similar results were also reported by Majeed et al. [51] On the other hand polarity of the starch after US treatment is dependent upon degradation of starch into hydrophilic groups including monosaccharides and disaccharides that have higher affinity for water than starch, thus increasing the water absorption capacity of starch [52]. As evident from our results both the functional properties displayed significant increase ($p \leq 0.05$), hence we conclude that increased polarity after US treatment displayed no significant effect on OAC.

**Table 3**
Functional properties of untreated and US-treated resistant starch from lotus stem.

| Sample | RS | URS1 | URS2 | URS3 | URS4 |
|---|---|---|---|---|---|
| US power | – | 100 W | 200 W | 300 W | 400 W |
| WAC (g/g) | 0.50 ± 0.76$^{a}$ | 1.23 ± 0.98$^{b}$ | 2.11 ± 1.89$^{c}$ | 2.87 ± 0.43$^{c}$ | 3.53 ± 1.12$^{d}$ |
| OAC (g/g) | 0.22 ± 0.76$^{a}$ | 1.09 ± 0.23$^{b}$ | 1.79 ± 1.29$^{b}$ | 2.87 ± 0.55$^{c}$ | 2.93 ± 0.24$^{c}$ |
| Freeze thaw stability (%) | | | | | |
| 0 thaw | 3.18 ± 0.12$^{c}$ | 2.87 ± 0.87$^{b}$ | 1.98 ± 0.86$^{a}$ | 1.26 ± 1.34$^{a}$ | 1.09 ± 0.45$^{a}$ |
| 1 thaw | 4.12 ± 1.98$^{c}$ | 2.99 ± 0.12$^{b}$ | 2.50 ± 0.28$^{b}$ | 1.76 ± 0.54$^{a}$ | 1.34 ± 0.78$^{a}$ |
| 2 thaw | 10.76 ± 1.07$^{c}$ | 5.16 ± 1.90$^{b}$ | 4.07 ± 0.57$^{a}$ | 5.21 ± 0.89$^{b}$ | 4.54 ± 1.09$^{a}$ |
| 3 thaw | 13.09 ± 0.54$^{c}$ | 10.78 ± 0.23$^{a}$ | 11.76 ± 0.19$^{b}$ | 12.35 ± 0.92$^{b}$ | 10.65 ± 0.65$^{a}$ |
| 4 thaw | 19.10 ± 0.32$^{d}$ | 17.89 ± 0.35$^{c}$ | 15.49 ± 1.23$^{b}$ | 13.07 ± 1.23$^{a}$ | 13.75 ± 1.23$^{a}$ |
| 5 thaw | 23.10 ± 1.10$^{d}$ | 20.76 ± 1.29$^{c}$ | 19.23 ± 1.11$^{b}$ | 17.22 ± 0.24$^{a}$ | 16.43 ± 0.85$^{a}$ |

Where WAC is the water absorption capacity; OAC is the oil absorption capacity; US is ultrasonication; URS1, URS2, URS3 and URS4 represent the resistant starch ultrasonicated at 100, 200, 300 and 400 W. The results are the means of three replications ± standard deviations. Means in the row with different superscript differ significantly ($p > 0.05$).

### 3.6. Freeze thaw stability

The freeze thaw stability of starch is an important parameter that measures the stability of starch during freezing and decides its use in frozen food products. It is measured as the percentage of water released (syneresis) during a freeze thaw cycle. In our study all the samples were subjected to five cycles of freezing and thawing. The percent syneresis of all the samples increased after fifth cycle and displayed the lowest values of freeze thaw stability (Table 3). This may be attributed to the interaction of amylopectin with the leached amylose chains that forms the junction zones and ooze out water upon storage [53]. However the percent syneresis of US treated samples was significantly lower ($p < 0.05$) than RS (Table 2). The reason may be the that US results in damage to the hydrogen bonding which exposes the hydroxyl groups located inside the double helices to the surrounding water. This may enhance their interaction with water and increase their water retaining capacity. A similar observation on freeze–thaw stability of maize starch subjected to ultrasonic treatment was made by Hu et al. [54].

### 3.7. Effect on anti-oxidant potential

US treatment can play a great role in modifying the biological activities including anti-inflammatory, antioxidant, and anticancer activities of biopolymers [55]. The effect of US on the anti-oxidant activity of RS was investigated by determining the radical scavenging activities of 2, 2-diphenyl-1-picrylhydrazyl (DPPH) and the detection of metal chelating activity. DPPH radical scavenging activity of RS was found to be 18.87 ± 0.90% (Fig. 4A). The values increased significantly ($p < 0.05$) with the increase in US power (100–400 W), with the values of inhibition ranging from 23.37 ± 1.23 to 37.45 ± 0.70%. The activity was however low as compared to the positive control (α-tocopherol). Antioxidant activity of RS is due to its hydroxyl group [22]. The antioxidant potential of polysaccharides depends on the number of free hydroxyl groups in their molecules [56]. The increase in DPPH scavenging activity could be attributed to the breaking of hydrogen bonds during ultrasonic treatment. The breakage of bonds might expose more hydroxyl groups in treated polysaccharide which can allow more scavenging of DPPH radicals [57]. The metal chelating activity of the US treated samples (Fig. 4 B) was also significantly higher ($p < 0.05$) than RS. Metal chelating activity of RS showed a value of 21. 71 ± 1.41% whereas US treated samples displayed values ranging 25.16 ± 1.03 to 40.56 ± 1.60% for the sonication power increasing from 100 to 400 W. The reason may again be attributed to the exposure of hydroxyl groups after US. Our findings are in accordance with Yan et al. [58] who reported that scavenging activity of yellow tea polysaccharides increased with US due to the increase in hydroxyl groups. Ultrasonic treatment yields lower molecular weight polysaccharides that will have more free hydroxyl groups and higher contents of reducing sugars at the same mass concentration, thereby exerting stronger hydrogen-donating ability [59]. Yuan et al. [60] also reported the improvenment in the bioactivity (anti-oxidant potential) of polysaccharide from *Sargassum pallidum* after ultrasonic treatment.

### 3.8. Bile acid binding capacity

Bile acids (BA) are synthesized from cholesterol in the liver and majority of these are reabsorbed by terminal ileum after emulsification with fat in small intestine. However the other possible mechanism of elimination of bile acids from intestine is the entrapment of bile by dietary fibre thus increasing faecal bile acid excretion which in turn leads

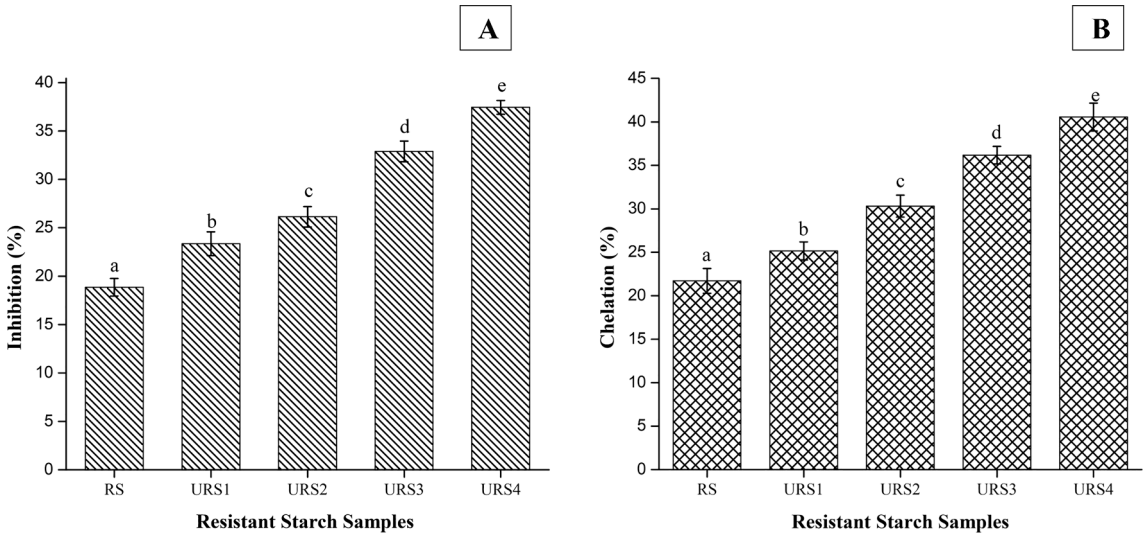


**Fig. 4.** Antioxidant potential of untreated and ultrasonication treated resistant starch from lotus stem A) DPPH Scavenging activity, B) Metal chelating activity.

**Table 4**
In vitro bile acid binding and pancreatic lipase inhibiting activity of untreated and US-treated resistant starch from lotus stem.

| Sample | Power (W) | Bile acid binding capacity (%) | Lipase inhibition (%) |
|---|---|---|---|
| RS | – | 8.45 ± 0.09[a] | 34.09 ± 0.10[a] |
| URS1 | 100 | 10.11 ± 0.45[b] | 39.10 ± 0.34[b] |
| URS2 | 200 | 11.45 ± 0.16[c] | 46.23 ± 0.43[c] |
| URS3 | 300 | 12.09 ± 1.29[d] | 52.09 ± 1.20[d] |
| URS4 | 400 | 16.14 ± 0.96[e] | 56.11 ± 0.98[e] |

Where US represent ultrasonication; URS1, URS2, URS3 and URS4 represent resistant starch ultrasonicated at 100, 200, 300 and 400 W. The results are the means of three replications ± standard deviations. Means in the column with different superscript differ significantly ($p > 0.05$).

to reduction of blood cholesterol [61]. The BA binding capacity of RS was observed to be 8.45 ± 0.09% whereas for US treated samples, the values ranged from 10.11 ± 0.45% to 16.14 ± 0.96% (Table 4). A significant increase ($p < 0.05$) among the results of BA binding capacities with the increase in frequency of US was seen. BA binding capacity of RS may be due to the presence of helical structure in RS which results in lower BA concentration in supernatant [62]. It is the hydrophobic interior of these helical structures (formed by 1, 4-linked glucose units of amylose and amylopectin) that act as the binding site for amphiphilic ligand [63]. The degree of this binding depends upon the stability of RS matrix and the number of sites per unit. The loose interior structure of RS might enhance its BA binding capacity [64]. As the frequency of US treatment increases, the surface of RS may develop more cracks which will allow BA (especially dihydroxy-BA) to enter through the cracks developed and increase bile binding capacity. The effect of loose matrix of pea resistant starch on BA capacity was also reported by Zhou, Ma, Xu, Li and Hu, 2019 [64] . The interaction of two hydroxyl groups in the deoxycholic acid molecule with the hydroxyl group in starch is stronger [65]. Subsequently as the US power increases, more will be exposure of hydroxyl groups in RS and more will be the BA binding potential. As the sonication power of URS4 displayed maximum BA binding capacity, so it can be assumed to have maximum cholesterol lowering potential.

### 3.9. Effect on anti-lipidemic activity.

The anti-lipidemic property of RS and US treated samples was determined in terms of pancreatic lipase inhibition activity. Pancreatic lipase (PL) is the most important enzyme involved in triglyceride digestion. The delay or suppression of PL is a key approach to lower obesity and hyperlipidaemia as the inhibition of PL influences triglyceride digestion and absorption [66]. Resistant starch has been reported to lower blood lipids especially triglycerides and cholesterol [67]. The value of PL inhibition of RS was found to be 34.09 ± 0.10 and that of US treated samples increased from 39.10 ± 0.34% to 56.11 ± 0.98%. The significant increase ($p < 0.05$) in PL inhibition activity with the increase in US power can be attributed to the breakdown of RS matrix which increases the accessibility of PL to RS matrix. As displayed by SEM results, the compact and smooth surface of short chain amylose crystallite of RS can hinder the accessibility of enzyme to the matrix [68], whereas US breaks down the matrix resulting in enhanced enzyme substrate interaction. In our study as the ultrasound power increased, the PL inhibitory activity of RS increased. Ultrasonication method was also found to increase the PL inhibitory activity of *A. malaccensis* and *A. subintegra* leaves due to reduction of particle diameters by the cavitation energy generated by ultrasound [69]. Similarly, soluble dietary fibre (SDF) from lotus root nodules subjected to micronization (size reduction) were also investigated for PL inhibition and it was observed that micronized powders had more PL inhibition as compared to non –micronized powders [66]. The micronized powders had more binding sites for PL with carboxyl groups exhibiting more inhibition on PL. In our study, the variation in particle size and structure induced by US may contribute to the increased PL inhibition by RS.

### 3.10. In vitro glycemic index

In vitro hydrolysis of RS and US treated samples was carried out to evaluate the % of starch digested during the given period of time. The results are presented in Table 5. The rate of hydrolysis and glycemic index (GI) was highest for white bread (% hydrolysis of 50.07 ± 1.33 and glycemic index of 67.19 ± 0.96) and lowest for RS (% hydrolysis of 23.11 ± 1.09 and glycemic index of 52.39 ± 0.38). For US treated samples, as the sonication power increased from 100 to 400 W, GI increased. The US treatment of samples increased the values of hydrolysis from 38.12 to 46.45% and GI from 59.43 to 65.09%, indicating that ultrasound assisted in fragmentation of resistant starch surface and induced a disruption in the spatial arrangement of starch crystalline structure [29]. The resulting RS granules became more susceptible to enzymatic action which increased the glycemic index [70]. Our results are supported by the study carried out by Kunyanee and Luangsaku [71] who also reported an increase in GI after application of ultrasound, in case of rice starch. Apart from these factors, hydrolysis of starch by enzymes is also governed by amylose content, gelatinization enthalpy relative crystallinity and gelatinization temperature [72]. The classification of foods on the basis of GI includes low GI food (GI of 55), medium GI food (GI of 56–69) and high GI foods (GI of 70) [73]. For RS the low GI values can be an important nutritional property as studies have reported that low GI/ high RS foods prevents cardiovascular and cerbrovascular diseases, regulates blood glucose level, decreases insulin resistance, and improves lipid metabolism [74]. We assert that as GI of the US treated samples were found to be high as compared to native RS, this may have a profound physiological impact on blood glucose. It might be speculated that US treated samples can increase glycemic risk when consumed over time and may not be useful for control of blood glucose in the management of diabetic patients. However more in depth in vitro and in vivo studies need to be carried out to probe the effect of ultrasonication on the decreased resistance to the digestibility of resistant starch and higher GI.

## 4. Conclusions

Ultrasound processing of resistant starch (RS) induced some modifications in its size, morphology, functional properties, bile acid binding, anti-oxidant potential, pancreatic Lipase binding ability and in vitro glycemic index. The magnitude of these changes varied with the power of ultrasound. Ultrasound resulted in a decrease of particle size and caused disintegration of the RS matrix resulting in small particles of irregular shape. Freeze thaw stability, water and oil absorption capacity increased with the increase in ultrasound power. In terms of nutraceutical properties, bile acid binding, anti-oxidant potential, pancreatic lipase binding activity increased with the increase in ultrasound power depicting that US treatment can be used to enhance the nutraceutical potential of RS. However, the process resulted in an increased percent hydrolysis (%) and glycemic index. The results obtained indicate that

**Table 5**
Calculated hydrolysis index (HI) and predicted glycemic index (GI) for untreated and US treated resistant starch from lotus stem.

| Sample | Power | HI (%) | GI (%) |
|---|---|---|---|
| White bread | – | 50.07 ± 1.33[f] | 67.19 ± 0.96[e] |
| RS | – | 23.11 ± 1.09[a] | 52.39 ± 0.38[a] |
| URS1 | 100 | 26.34 ± 0.36[b] | 54.17 ± 1.08[b] |
| URS2 | 200 | 29.63 ± 1.21[c] | 55.97 ± 0.23[b] |
| URS3 | 300 | 32.09 ± 1.43[d] | 57.32 ± 1.26[c] |
| URS4 | 400 | 36.06 ± 0.13[e] | 59.50 ± 0.11[d] |

Where US represent ultrasonication; URS1, URS2, URS3 and URS4 represent resistant starch ultrasonicated at 100, 200, 300 and 400 W; HI is hydrolysis index; and GI is glycemic index. The results are the means of three replications ± standard deviations. Means in the column with different superscript differ significantly ($p > 0.05$).

ultrasound can be an eco-friendly and facile technique, which allows physical, morphological and nutraceutical modifications of resistant starch isolated from lotus stem for different potential applications.

## CRediT authorship contribution statement

**Nairah Noor:** Investigation, Writing - original draft. **Adil Gani:** Supervision, resources & Conceptulization. **Faiza Jhan:** Formal analysis. **J.L.H. Jenno:** Writing - review & editing. **Mohd Arif Dar:** Software.

## Declaration of Competing Interest

The authors declare that they have no known competing financial interests or personal relationships that could have appeared to influence the work reported in this paper.

## Acknowledgements

Dr Adil Gani is thankful to DST, INSPIRE programme, Government of India for the award of Junior Research Fellowship (No: DST/INSPIRE Fellowship/[IF180189]) to his scholar Miss Nairah Noor.

## References

[1] H. Englyst, H.S. Wiggins, J.H. Cummings, Determination of the non-starch polysaccharides in plant foods by gas-liquid chromatography of constituent sugars as alditol acetates, Analyst 107 (1272) (1982) 307, https://doi.org/10.1039/an9820700307.
[2] H.N. Englyst, S.M. Kingman, J.H. Cummings, Classification and measurement of nutritionally important starch fractions, Eur. J. Clin. Nutr. 46 (Suppl 2) (1992) S33–S50.
[3] A. Salehi-Abargouei, R. Ghiasvand, M. Hariri, Prebiotics, prosynbiotics and synbiotics: can they reduce plasma oxidative stress parameters? A Systematic Review. 9 (2017) 1–11.
[4] K.L. Johnston, E.L. Thomas, J.D. Bell, G.S. Frost, M.D. Robertson, Resistant starch improves insulin sensitivity in metabolic syndrome, Diabet. Med. 27 (2010) 391–397.
[5] K.C. Maki, C.L. Pelkman, E.T. Finocchiaro, K.M. Kelly, A.L. Lawless, A.L. Schild, T. M. Rains, Resistant starch from high-amylose maize increases insulin sensitivity in overweight and obese men, J. Nutr. 142 (2012) 717–723.
[6] X. Si, P. Strappe, C. Blanchard, Z. Zhou, Enhanced anti-obesity effects of complex of resistant starch and chitosan in high fat diet fed rats, Carbohydr. Polym. 157 (10) (2017) 834–841.
[7] D.F. Birt, T. Boylston, S. Hendrich, J.L. Jane, J. Hollis, L. Li, J. McClelland, S. Moore, G.J. Phillips, M. Rowling, K. Schalinske, M.P. Scott, E.M. Whitley, Resistant starch: promise for improving human health, Adv. Nutr. 4 (2013) 587–601.
[8] Q. Kuang, J. Xu, K. Wang, S. Zhou, X. Liu, Structure and digestion of hybrid indica rice starch and its biosynthesis, Int. J. Biol. Macromol. 93 (2016) 402–407.
[9] B. Zhang, S. Dhital, B.M. Flanagan, P. Luckman, P.J. Halley, M.J. Gidley, Extrusion induced low-order starch matrices: enzymic hydrolysis and structure, Carbohyd. Polym. 134 (2015) 485–496.
[10] Q. Xia, L. Wang, Y. Li, Exploring high hydrostatic pressure-mediated germination to enhance functionality and quality attributes of wholegrain brown rice, Food Chem. 249 (2018) 104–110.
[11] T.-T. Huang, D.-N. Zhou, Z.-Y. Jin, X.-M. Xu, H.-Q. Chen, Effect of repeated heat-moisture treatments on digestibility, physicochemical and structural properties of sweet potato starch, Food Hydrocoll. 54 (2016) 202–210.
[12] M. Li, J. Li, C. Zhu, Effect of ultrasound pretreatment on enzymolysis and physicochemical properties of corn starch, Int. J. Biol. Macromol. 111 (2018) 848–856.
[13] A.S. Babu, R.J. Mohan, R. Parimalavalli, Effect of single and dual-modifications on stability and structural characteristics of foxtail millet starch, Food Chem. 271 (2019) 457–465.
[14] Q.-Y. Yang, X.-X. Lu, Y.-Z. Chen, Z.-G. Luo, Z.-G. Xiao, Fine structure, crystalline and physicochemical properties of waxy corn starch treated by ultrasound irradiation, Ultrason. Sonochem. 51 (2019) 350–358.
[15] M. Sujka, Ultrasonic modification of starch — impact on granules porosity, Ultrason. Sonochem. 37 (2017) 424–429.
[16] Y. Ding, Y. Xiao, Q. Ouyang, F. Luo, Q. Lin, Modulating the in vitro digestibility of chemically modified starch ingredient by a non-thermal processing technology of ultrasonic treatment, Ultrason. Sonochem. 70 (2021), 105350.
[17] Y.i. Zhang, X.u. Lu, S. Zeng, X. Huang, Z. Guo, Y. Zheng, Y. Tian, B. Zheng, Nutritional composition, physiological functions and processing of lotus (*Nelumbo nucifera Gaertn.*) seeds: a review, Phytochem Rev. 14 (3) (2015) 321–334.
[18] M. Ahmad, S. Qureshi, S. Maqsood, A. Gani, F. Masoodi, Micro-encapsulation of folic acid using horse chestnut starch and β-cyclodextrin: Microcapsule characterization, release behavior & antioxidant potential during GI tract conditions, Food Hydrocoll. 66 (2017) 154–160.
[19] A. Gani, B.A. Ashwar, G. Akhter, A. Gani, A. Shah, F.A. Masoodi, I.A. Wani, Resistant starch from five Himalayan rice cultivars and Horse chestnut: extraction method optimization and characterization, Sci. Rep. 10 (2020) 4097.
[20] AACC, Approved Methods of the AACC International, Methods 44–17, 76–13, 08–16, 32–40 and 35–05, 10th ed., The Association AACC, St. Paul, MN, 2000.
[21] M. Ahmad, A. Gani, F.A. Masoodi, S.H. Rizvi, Influence of ball milling on the production of starch nanoparticles and its effect on structural, thermal and functional properties, Int. J. Biol. Macromol. 151 (2020) 85–91.
[22] B.A. Ashwar, A. Gani, I.A. Wani, A. Shah, F.A. Masoodi, D.C. Saxena, Production of resistant starch from rice by dual autoclaving retrogradation treatment: Invitro digestibility, thermal and structural characterization, Food Hydrocoll. 56 (2016) 108–117.
[23] F. Jhan, A. Shah, A. Gani, M. Ahmad, N. Noor, Nano-reduction of starch from underutilised millets: effect on structural, thermal, morphological and nutraceutical properties, Int. J. Biol. Macromol. 159 (2020) 1113–1121.
[24] A. Shah, F.A. Masoodi, A. Gani, B.A. Ashwar, Effect of γ-irradiation on antioxidant and antiproliferative properties of oat β-glucan, Radiat Phys. Chem. 117 (2015) 120–127.
[25] S.K. Reshmi, M.L. Sudha, M.N. Shashirekha, Starch digestibility and predicted glycemic index in the bread fortified with pomelo (Citrus maxima) fruit segments, Food Chem. 237 (2017) 957–965.
[26] I. Goni, A. Garci-Alonso, B. Suara-Calirto, Starch hydrolysis procedure to estimate glycemic index, Food Nutr. Res. 17 (1997) 427–437.
[27] V. Badmaev, Y. Hatakeyama, N. Yamazaki, A. Noro, F. Mohamed, C.T. Ho, M. H. Pan, Preclinical and clinical effects of *Coleus forskohlii*, *Salacia reticulata* and *Sesamum indicum* modifying pancreatic lipase inhibition in vitro and reducing total body fat, J. Funct. Foods. 15 (2015) 44–51.
[28] F.O. Ogutu, T.H. Mu, Ultrasonic degradation of sweet potato pectin and its antioxidant activity, Ultrason. Sonochem. 38 (2017) 726–734.
[29] F. Zhu, Impact of ultrasound on structure, physicochemical properties, modifications, and applications of starch, Trends Food Sci. Technol. 43 (1) (2015) 1–17.
[30] M. Sujka, J. Jamroz, Ultrasound-treated starch: SEM and TEM imaging, and functional behaviour, Food Hydrocoll. 31 (2013) 413–419.
[31] E. Hasanvand, M. Fathi, A. Bassiri, M. Javanmard, R. Abbaszadeh, Novel starch based nanocarrier for vitamin D fortification of milk: production and characterization, Food Bioprod Process. 96 (2015) 264–277.
[32] A. Blennow, A. Mette Bay-Smidt, R. Bauer, Amylopectin aggregation as a function of starch phosphate content studied by size exclusion chromatography and on-line refractive index and light scattering, Int. J. Biol. Macromol. 28 (5) (2001) 409–420.
[33] I. Ullah, T. Yin, S. Xiong, Q. Huang, J. Zhang, A.B. Javaid, Effects of thermal pretreatment n physicochemical properties of nano-sized okara (soybean residue) insoluble dietary fiber prepared by wet media milling, J. Food Eng. 237 (2018) 18–26.
[34] L. Dai, C. Li, J. Zhang, F. Cheng, Preparation and characterization of starch nanocrystals combining ballmilling with acid hydrolysis, Carbohydr. Polym. 180 (2018) 122–127.
[35] S. Honary, F. Zahir, Effect of zeta potential on the properties of nano-drug delivery systems - A review (Part 2). 12 (2013) 265-273.
[36] Z. Ma, X. Yin, X. Hu, X. Li, L. Liu, I. Joyce, J.I. Boye, Structural characterization of resistant starch isolated from Laird lentils (*Lens culinaris*) seeds subjected to different processing treatments, Food Chem. 263 (2018) 163–170.
[37] J.J.G.V. Soest, H. Tournois, D.D. Wit, J.F.G. Vliegenthart, Short-range structure in (partially) crystalline potato starch determined with attenuated total reflectance Fourier transform IR spectroscopy, Carbohydr. Res. 279 (95) (1995) 201–214.
[38] D. Yongbo, Y. Xiao, Q. Ouyang, F. Luo, Q. Lin, Modulating the in vitro digestibility of chemically modified starch ingredient by a non-thermal processing technology of ultrasonic treatment, Ultrason Sonochem. 70 (2021), 105350.
[39] A.N. Dundar, D. Gocmen, Effects of autoclaving temperature and storing time on resistant starch formation and its functional and physicochemical properties, Carbohydr. Polym. 97 (2013) 764–771.
[40] X. Kang, P. Liu, W. Gao, Z. Wu, B. Yu, R. Wang, B. Cui, L. Qiu, C. Sun, Preparation of starch-lipid complex by ultrasonication and its film forming capacity, Food Hydrocoll. 99 (2020), 105340.
[41] Y. Li, Z. Wu, N. Wan, X. Wang, M. Yang, Extraction of high-amylose starch from *Radix Puerariae* using high-intensity low-frequency ultrasound, Ultrason. Sonochem. 59 (2019), 104710.
[42] M. Lopez-Silva, L.A. Bello-Perez, V.M. Castillo-Rodriguez, E. Agama-Acevedo, J. Alvarez-Ramirez, In vitro digestibility characteristics of octenyl succinic acid (OSA) modified starch with different amylose content, Food Chem. 304 (2020), 125434.
[43] AOAC, Official Methods of Analysis, Association of official Analytical chemistry, Airlington, 1990.
[44] A.M. Hermansson, K. Svegmark, K. Developments in the understanding of starch functionality, Trends Food Sci. Technol. 7(1996) 345-353.
[45] A. Li, Q. Gao, R. Ward, Physicochemical properties and in vitro digestibility of resistant starch from mung bean (*Phaseolus radiatus*) starch, Starch/Starke 63 (2011) 171–178.
[46] J.H. Dupuis, Q. Liu, R.Y. Yada. Methodologies for increasing the resistant starch content of food starches: a review, Comprehe. Rev. Food Sci. Food Safety 13(2014) 1219-1234.
[47] H. Wang, K. Xu, Y. Ma, Y. Liang, H. Zhang, L. Chen, Impact of ultrasonication on the aggregation structure and physicochemical characteristics of sweet potato starch, Ultrason. Sonochem. 63 (2020), 104868.

[48] J.E. Kinsella, N. Melachouris, Functional properties of proteins in foods: a survey, Crit. Rev. Food Sci. Nutr. 7 (3) (1976) 219–280.
[49] R. Singh, V.S. Sharanagat, Physico-functional and structural characterization of ultrasonic-assisted chemically modified elephant foot yam starch, Int. J. Biol. Macromol. 164 (2020) 1061–1069.
[50] J.O. Abu, K.G. Duodu, A. Minnaar, Food Chem. 95 (2006) 386–393.
[51] T. Majeed, I.A. Wani, P.R. Hussain, Effect of dual modification of sonication and γ-irradiation on physicochemical and functional properties of lentil (*Lens culinaris L.*) starch, Int. J. Biol. Macromol. 101 (2017) 358–365.
[52] H.J. Chung, R. Hoover, Q. Liu, Int. J. Biol. Macromol. 44 (2009) 203–210.
[53] C. Perera, R. Hoover, Food Chem. 64 (1999) 361–375.
[54] A. Hu, L. Li, J. Zheng, J. Lu, X. Meng, Y. Liu, R.U. Rehman, Different-frequency ultrasonic effects on properties and structure of corn starch, J. Sci. Food Agric. 94 (14) (2014) 2929–2934.
[55] X. Wang, M. Majzoobi, A. Farahnaky, Ultrasound-assisted modification of functional properties and biological activity of biopolymers: a review, Ultrason. Sonochem. 65 (2020) 105057, https://doi.org/10.1016/j.ultsonch.2020.105057.
[56] W. Li, X. Jiang, P. Xue, S. Chen, Inhibitory effects of chitosan on superoxide anion radicals and lipid free radicals, Sci. Bull. 47 (2002) 887–889.
[57] O.P. Sharma, T.K. Bhat, DPPH antioxidant assay revisited, Food Chem. 113 (4) (2009) 1202–1205.
[58] J.K. Yan, Y.Y. Wang, H.L. Ma, Z.B. Wang, Ultrasonic effects on the degradation kinetics, preliminary characterization and antioxidant activities of polysaccharides from *Phellinus linteus* mycelia, Ultrason. Sonochem. 29 (2016) 251–257.
[59] D. Yuana, C. Lia, Q. Huang, X. Fua, Ultrasonic degradation effects on the physicochemical, rheological and antioxidant properties of polysaccharide from Sargassum pallidum, Carbohydr. Polym. 239 (2020), 116230.
[60] X. Guo, X. Ye, Y. Sun, D. Wu, N. Wu, Y. Hu, S. Chen, Ultrasound effects on the degradation kinetics, structure, and antioxidant activity of sea cucumber fucoidan, J. Agric. Food Chem. 62 (5) (2014) 1088–1095.
[61] I.Y. Bae, S. Lee, S.M. Kim, H.G. Lee, Effect of partially hydrolysed oat bglucan on the weight gain and lipid profile of mice, Food Hydrocoll. 23 (2009) 2016–2021.
[62] M. Soral-Smietana, M. Wronkowsa, Resistant starch – nutritional and biological activity, Polish J. Food Nutr. Sci. 13 (2004) 51–64.
[63] C. Abadie, M. Hug, C. Kubli, N. Gains, Effect of cyclodextrins and undigested starch on the loss of chenodeoxycholate in the faeces, Biochem. 299 (1994) 725–730.
[64] D. Zhou, Z. Ma, J. Xu, X. Li, X. Hu, Resistant starch isolated from enzymatic, physical, and acid treated pea starch: preparation, structural characteristics, and in vitro bile acid capacity, LWT 116 (2019) 10854.
[65] K. Zhou, W. Xia, C. Zhang, L. (Lucy) Yu, In vitro binding of bile acids and triglycerides by selected chitosan preparations and their physico-chemical properties, LWT 39 (10) (2006) 1087–1092.
[66] H. Chen, J. Lia, R. Yao, S. Yan, Q. Wang, Mechanism of lipid metabolism regulation by soluble dietary fibre from micronized and non-micronized powders of lotus root nodes as revealed by their adsorption and activity inhibition of pancreatic lipase, Food Chem. 305 (2020), 125435.
[67] N. Nia, L. Shena, X. Lina, L. Zhao, Y. Hong, Y. Feng, Review on characteristics of resistant starch in traditional chinese medicine based on the theory of 'unification of medicines and excipients, NAPDD 5 (2020), 555662.
[68] Z. Wei, Y. Huaping, Z. Huanxin, Preparation and thermodynamic analysis of ginkgo resistant starch by ultrasonic-acid hydrolysis, Food Sci. Technol. 43 (2018) 293–299.
[69] M.N.M. Rodhi, F. Hamzah, K. Halim, K. Hamid, Kinetic behaviour of pancreatic lipase inhibition by Ultrasonicated *A. malaccensis* and *A. subintegra* leaves of different particle sizes, Bull. Chem. React. Eng. 15 (2020) 818–828.
[70] Y. Ding, J. Zheng, X. Xia, T. Ren, J. Kan, Preparation and characterization of resistant starch type IV nanoparticles through ultrasonication and miniemulsion cross-linking, Carbohydr. Polym. 141 (2016) 151–159.
[71] K. Kunyanee, N. Luangsakul, The effects of ultrasound – assisted recrystallization followed by chilling to produce the lower glycemic index of rice with different amylose content, Food Chem. 323 (2020), 126843.
[72] H.J. Chung, Q. Liu, R. Hoover, Impact of annealing and heat-moisture treatment on rapidly digestible, slowly digestible and resistant starch levels in native and gelatinized corn, pea and lentil starches, Carbohydr. Polym. 75 (3) (2009) 436–447.
[73] D.J.A. Jenkins, C.W.C. Kendall, T.H. Nguyen, A. Marchie, D.A. Faulkner, C. Ireland, A.R. Josse, E. Vidgen, E.A. Trautwein, K.G. Lapsley, C. Holmes, R.G. Josse, L. A. Leiter, P.W. Connelly, W. Singer, Effect of plant sterols in combination with other cholesterol lowering foods, Metabolism 57 (1) (2008) 130–139.
[74] C. Chung, L. Sanguansri, M.A. Augustin, Resistant starch modification: effects on starch properties and functionality as co-encapsulant in sodium caseinate based fish oil microcapsules, J. Food Sci. Technol. 75 (2010) E636–E642.